XL CILAMCE
IBERO-LATIN AMERICAN CONGRESS ON COMPUTATIONAL METHODS IN ENGINEERING
NOVEMBER 11-14, 2019
Praiamar Natal Hotel & Convention
Natal, RN-BRAZIL

DIFFERENT STRUCTURAL MONITORING TECHNIQUES IN LARGE RC BUILDING: A CASE STUDY

Marcos A. Silva
Andreia R. Fanton
Luiz C. Almeida
Leandro M. Trautwein
Maria Teresa Françoso
Irving P. Marchena
marcos@fec.unicamp.br
University of Campinas
Cidade Universitária "Zeferino Vaz", 13083-970, São Paulo, Brazil

Abstract.

Civil construction area is in continuous technological evolution, either related to new material and execution techniques or development of analytical and design methods. In Brazil, particularly, standard codes have been created and updated in the last 10 years due to new studies related to a better behavior of concrete structures, i.e., ABNT NBR 15961 (2011), NBR 16055 (2012), NBR 15575 (2013), NBR 6118 (2014), etc. These standard codes are fundamental to ensure the safety of structures, qualifying them for their use. Nowadays, however, it is still able to find recent buildings with obvious pathologies which are consequence of error and mistakes in different stages of the construction and might cause the building interdiction or even collapse. Excessive displacements and crack openings in reinforced concrete constructions represents examples of pathology and require structural intervention to eliminate or mitigate these effects. After the pathologies correction, it is important to verify the structural behavior regarding to acting forces, in order to ensure safety and the correct structural performance. In this paper, a retrofit study was conducted in a large RC building after the structural intervention to correct some pathologies found. Vertical displacement of slabs and supporting beams was measured in specific points with auxiliary of dial gauges and precision geometric levelling as the load was applied in increments. In addition, numerical models were created using the computational programme TQS, which allowed for grid analogy method, in order to compare its results with experimental values. The results showed good agreement in terms of vertical displacement and structure behavior. It was possible to validate numerical results obtained by grid analogy and also certify both the safety and the performance of these structural elements.

Keywords: Monitoring, strengthening, RC structure, numerical analysis

1 Introduction

On-site visual inspections, non-destructive evaluation, structural health monitoring (SHM), and building pathology are different ways to quantify structural deterioration and guarantee the safety of structures (Napolitano et al. [1]). The health monitoring of structures consists of determining, by measured parameters, the location and severity of damage in buildings as they happen (Chang et al. [2]). As outlined in Almeida et al. [3], pathological problems in structures have specific manifestations, facilitating the identification of the origin and the mechanisms of the phenomena involved and the estimation of its consequences.

Since most of the pathological manifestations in buildings are related to construction stages - from project design to use of the structure -, durability and performance are aspects that must be guideline in the design of buildings. The appearance of some defects from enforcement proceedings may go unnoticed. The pathological manifestations come from conception and project mistakes, improper execution of the structure, misuse and lack of preventive maintenance. Therefore, these manifestations are mainly originated from human error (Araújo et al. [4]).

Pathology is a general term to describe the unsound, abnormal, generally undesirable phenomena. The documentation and the analysis of a structure are two key aspects of building pathology and diagnostics to understand the damage occurred and the effects to the stability (Napolitano et al. [5]).

Based on Carmo [6], building pathology can be understood as the engineering branch that studies the symptoms, causes and origins of constructive defects that arise in the construction of buildings. After the pathological manifestation, depending on the severity, the situation can migrate to failure which is the final consequence.

Helene [7] outlines five construction phases: planning, design, materials, execution and building use. Each step has its importance for the final result and to control pathological manifestation occurrence. The pathological problems are related to some mistake in at least one of these phases, and its occurrence is related to many symptoms or specific manifestations, exhibited during construction or building use, and may become evident at the beginning or after the end of construction (Almeida et al. [3]).

During the design phase, problems may arise from structural conception, analysis and design. Some mistakes are outlined by Souza and Ripper [8]: inadequate determination of the loads or combinations of actions; inadequate structural or analytical model; shortcoming in the design of the structure; lack of compatibility between the design of the structure and the architectonic and other projects; insufficient constructive details.

Regarding to pathologies that arise during the phase of execution of the structure, these may be related to the lack of skilled manpower and the lack of accompaniment of the responsible engineer to verify the construction and its activities.

Napolitano et al. [5] show that building pathology and diagnostics focus on the degradation and downfall of existing structures. The severity of pathologies can be quantified, the sources can be identified, and plans for intervention and prevention can be prioritized. The structural condition of an existing building can be assessed by assembling relevant data regarding and using computational modeling to simulate its response to loading conditions.

The main objective of this research is the retrofit study made in a large RC building after the structural intervention to correct same pathologies found. To do so, the new building of the Institute of Arts at the University of Campinas was studied. Vertical displacement of slabs and supporting beams was measured in specific points with auxiliary of dial gaugesand topography as the load was applied in increments.

The guidelines are: the numerical modelling of the structure using the computational programme TQS; the comparison between the numerical models and the experimental values; the validation of numerical results obtained by grid analogy; the certification of both the safety and the performance of the structural elements.

2 Building description

The building is a large structure designed to be a theater. It has two modules in which a considerable part is composed by reinforced concrete (RC), with the beams supporting flat slabs. The building closure was executed having RC wall with 250mm thickness. A great part of the internal beams are supported by RC columns.

Through the construction phase, it was identified some pathological manifestation due to several factors. Some of them resulting from poor execution, which leaded to missing important structural elements, and even questionable design conceptions of panel structures. In order to recover safety and serviceable conditions a strengthening process was performed with the inclusion of 8 circular steel columns. These columns increased the support conditions of first and second floor reducing the beam's span, and consequently its deflection.

3 Load tests

A load test was executed to verify if vertical displacements are inside the limit $l/350$ due to accidental load established by the brazilian standard ABNT NBR 6118 [9]. The first floor slab was incrementally filled with water simulating the load in which the floor would be subject.

Taking advantage of the inverted beams shuttering, a thin sand layer was deposited to rectify the first floor slab and covered with plastic canvas (see Figure 1). Afterwards, the water was pumped in three intervals (load steps) until it reached 15cm, 30cm and 50cm depth and the displacement read at the end of each one.

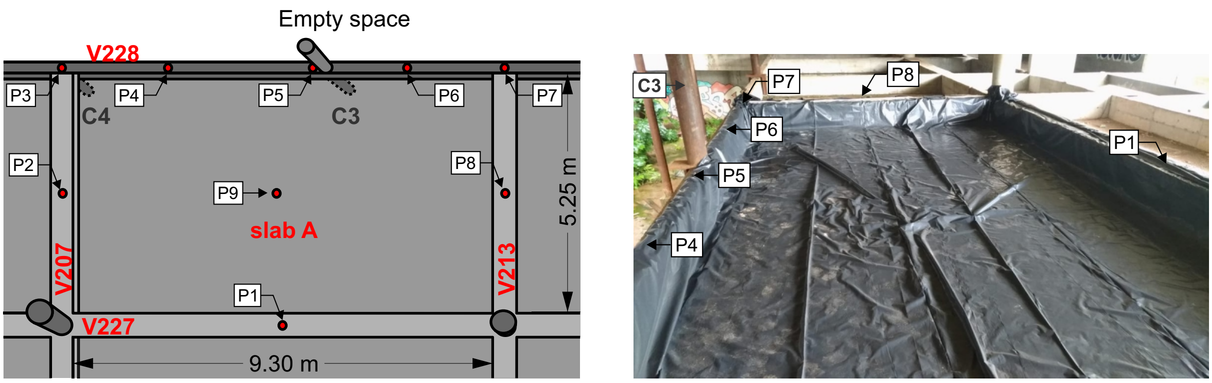

(a) (b)

Figure 1. Monitoring points in the first floor slab.

For monitoring, a Carl Zeiss model NI005A precision level with invar staff was used. Full details of its use were given in Marchena et al. [10]. As in accordance with the specifications, the level presents a standard deviation of $\pm$ 0.5mm/km in double-levelling, with compensating pendulum and parallel flat plate micrometre. The invar staff is double graduated (Left Reading (LR) and Right Reading (RR)) with 1.75 m height, equivalent intervals at dm/2 and divisions at each 5mm. The level-staff set allows uncertainty readings in tenths of a millimetre. Both monitoring points (P1 to P9) and reference level were marked with flat head bolts, fixed in the concrete to ensure observations were made on the same position. Figure 1a shows the position of monitoring points.

Analogical dial gauges Käfen with 0.01mm precision was also used to evaluate displacement. The equipment magnetic base was fixed on a steel frame structure built below the tested pavement. Hence, it had no interference in displacement readings through the loading process.

The dial gauge 1, which evaluated displacement on the first floor, was located in the inferior face of slab A, aligned with P9. Figure 2 shows the apparatus for displacement reading throughout the tests. These gauges worked as control points which were compared with topographic readings.

(a) Topograph (b) Dial gauge

Figure 2. Vertical displacement readings in the first floor test.

After finishing the first floor load test, the second floor slabs were prepared using equal procedure as the first one. Figure 3 shows the monitoring points employed in this case. However in this case, the loading process was divided into five intervals (load steps), the first three of it were applied on slab A while the last two on slab B. The medium water depth for intervals 1, 2 and 3 on slab A were 18cm, 34cm, 50cm, respectively. When slab A was filled, intervals 4 and 5 were applied in slab B with medium water depths 19cm and 46cm, respectively.

The dial gauge 2, which evaluated displacement on the second floor, was located in the inferior face of beam V324, aligned with monitor point P4. The support frame in this case was built in the first floor.

Figure 4 shows the loading procedure. When the water level reached certain depth, it had taken a 5-minute pause before the displacement measurements started. Thus, this was done to avoid possible interferences in the readings due to the water movement.

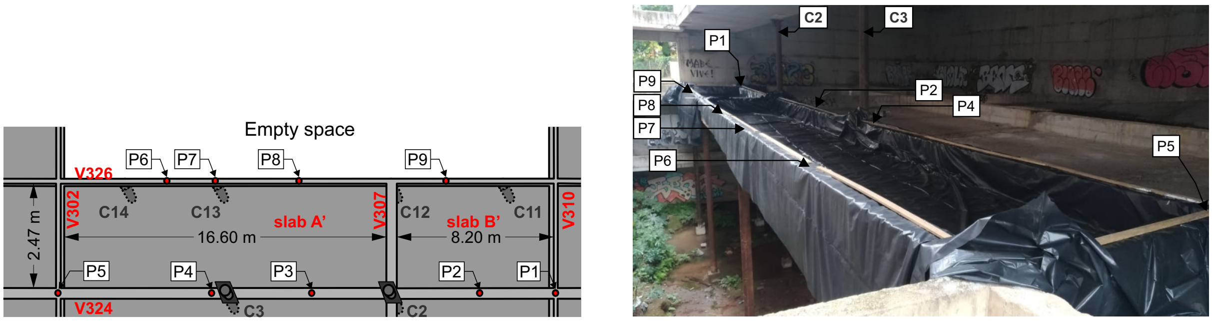

(a) (b)

Figure 3. Monitoring points in the second floor slabs.

(a) $1^{st} floor$ (b) $2^{nd} floor$

Figure 4. Loading test of the first and second floor.

4 Results

This section presents and discuss the results obtained from the load test performed on slab A at first floor, and slab A' and B' at the second floor. The vertical displacements were recorded in the corresponding load step mostly using precision geometric levelling. The dial gauge was employed in one specific point of each pavement. These displacements were related to the initial position, therefore they did not represent the absolute difference between load steps.

4.1 First floor

Table 1 shows the results for all monitoring point used in the first floor load test.

Table 1. Vertical displacement of the first floor monitors.

Monitoring Point	Load step displacement (mm) #1	#2	#3
P1	-0.17	-0.36	-0.61
P2	-0.16	-0.26	-0.29
P3	0.10	0.01	0.11
P4	-0.04	-0.19	-0.19
P5	-0.17	-0.14	-0.16
P6	-0.11	-0.17	-0.29
P7	-0.01	-0.15	-0.37
P8	-0.13	-0.10	-0.38
P9	-0.44	-0.71	-1.51
*P9	-0.34	-0.74	-1.47

* Dial gauge measurement

Three line axis were employed to analyze the structural behavior elements influenced by the load test. First one corresponds to the internal beam V227; second one passes through the center of slab A and is parallel to beam V227; the last one corresponds to external beam V228. The displacement pattern can be observed in Figure 5 for each load step. In general, the major deflections occurred near the center.

The V227 beam axis is supported by two circular concrete columns with high flexural and normal stiffness (see Figure 5a). Therefore, it is reasonable to conclude that these two points did not move throughout the load test. The middle span presented the major displacement (*P1*) achieving -0.61mm.

Similar behavior occurred in the central axis represented by the monitors *P2*, *P8* and *P9* (see Figure 5b). In this case, the beams supporting the slab are less rigid than columns, as result both edges moves downwards. The support condition affected the water distribution given that the levelling difference from load step 1 to 2 was positive and negative for monitors *P2* and *P8*, respectively. Also, the displacement magnitude when comparing load steps 2 and 3 was bigger on monitor *P8* than on *P2*. This happens because in the left side the beam V207 is simply supported in two columns; while on the right side V213 is simply supported in one column and another beam. The maximum deflection of the middle span (*P9*) was -1.51mm.

At the edge of the tested slab A, the V228 beam axis is supported by two columns (*C3* and *C4*) and one transversal beam (*V213*). Figure 5c illustrates the displacement pattern of this case. The influence of columns C3, C4, and the lack of direct support on the right portion became clear observing the deflected shape of V228 beam. Since the column C3 imposed a restriction, the vertical displacement at this position is admitted null. Initially, when small load was applied (step 1), the V228 axis behaved as a continuous beam with structural settling. The monitor *P5* was dislocated from column C3, hence it had its displacement reduced. The 0.10mm lifting observed in *Pt3* was not relevant and it is contained in the precision geometric levelling error.

As the load test continued (step 2), monitor *P3* and *P5* was practically held still while the others moved downwards. It was noted in load step 3 that the right portion of V228 beam axis experienced the major displacement. Also, no change was observed on the left span whereas the right portion moved. This could be caused by original crack condition of V228 beam preventing stress redistribution to the left portion. Monitor *P7* reached -0.37mm deflection.

Point *P9* was used to evaluate displacement at the slab middle span. Figure 5d shows the values obtained using the topographic equipment and the dial gauge 1. Overall, the results converged showing good agreement in the load steps. The relative difference between both monitoring techniques was below 0.1mm, which is the admissible error of the equipment.

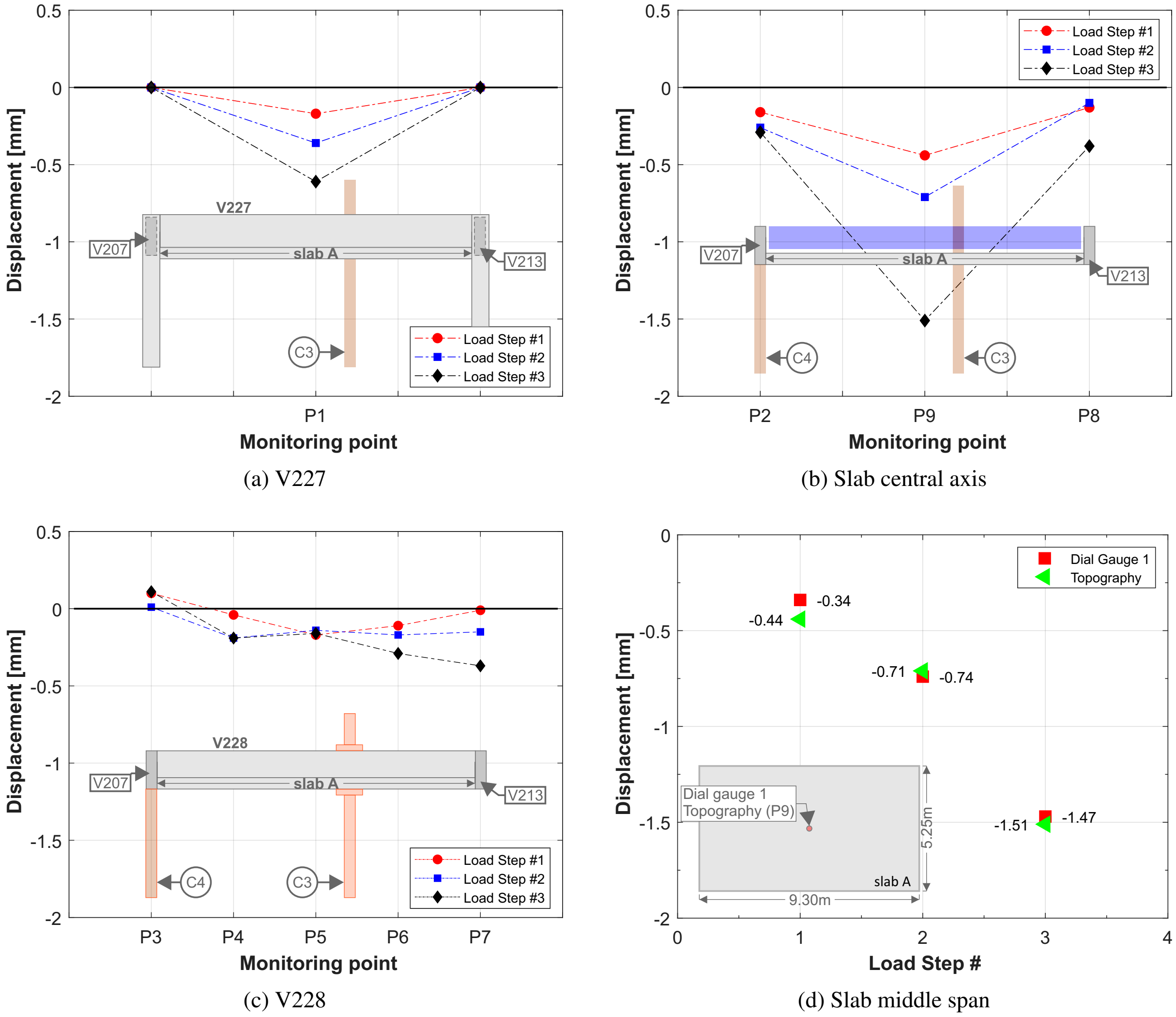

(a) V227

(b) Slab central axis

(c) V228

(d) Slab middle span

Figure 5. Measured displacements in the 1^{st} floor load test.

4.2 Second floor

Table 2 shows the results for all monitoring points used in the second floor load test.

Two line axis were employed to analyze the structural behavior of elements influenced by the load test. The first line corresponds to the internal beam V324 whereas the second corresponds to the external beam V326. Their displacement pattern are shown in Figure 6.

In the internal line axis (see Figure 6a) there are beams supporting slab A' and B'. Therefore, no monitor were kept in the original level and all monitors moved downwards. As the slab A' was being been loaded in steps 1 to 3, the monitors *P1* and *P2* remained practically immovable indicating that this process did not affect the slab B'. However, the displacement magnitude on the monitors *P3* to *P5* increased. When the slab A' was filled and the load started being applied on slab B' (steps 4 and 5), the displacement magnitude of the monitors *P1* and *P2* increased whereas in others it didn't happened. This indicates that loading slab B' did not have significant influence on slab A'. The major monitor displacement (-1.60mm) happened in *P4* which is near to the midspan of slab A'.

The external line axis is simply supported by four columns in the slabs A' and B' region (see Figure 6b). It was observed on monitor *P6* and *P8*, located at midspan of slab A', that the displacement enhanced throughout the three first load steps. The last two load steps were applied to the slab B' whilst slab A' had filled, thus its influence was not significant on monitors of slab A'. As expected, displacements of monitor *P7* located above column C13 can be neglected.

Table 2. Vertical displacement of the second floor monitors.

Monitoring Point	Load step displacement (mm) #1	#2	#3	#4	#5
P1	0.00	0.05	-0.01	-0.1	-0.25
P2	-0.12	-0.10	-0.14	-0.35	-0.73
P3	-0.46	-0.88	-1.35	-1.49	-1.58
P4	-0.37	-0.90	-1.57	-1.62	-1.60
*P4	-0.29	-0.77	-1.52	-1.58	-1.67
P5	-0.14	-0.66	-1.15	-1.20	-1.24
P6	-0.21	-0.35	-0.49	-0.55	-0.55
P7	0.00	-0.06	0.00	-0.04	-0.01
P8	-0.25	-0.40	-0.55	-0.48	-0.48
P9	0.01	-0.04	-0.06	-0.16	-0.16

* Dial gauge measurement

Monitor *P9* experienced a minor lifting at the initial load steps. There are two possible explanations for this effect being the first one related to equipment error involved. The second could be explained by a leverage effect that happened when monitor P8 moved down and column C12 remained fixed. By the end of the load test, when both slabs were filled in step 5, the structure settled and the monitor *P9* moved down -0.16mm. The major displacement registered -1.60mm occurred on monitor *P4*.

An attempt was made to keep dial gauge 2 aligned with monitor *P4* positioned in the bottom face of V324 beam. Figure 6c shows the displacement results using dial gauge and precision geometric levelling. It was noted good agreement in the measurements of all load steps. The major difference between both methods occurred on step 2 in which precision levelling absolute displacement was 0.13mm bigger than dial gauge reading. Looking at the last two load steps it become clear the effect of loading slab B' can be neglected on slab A'.

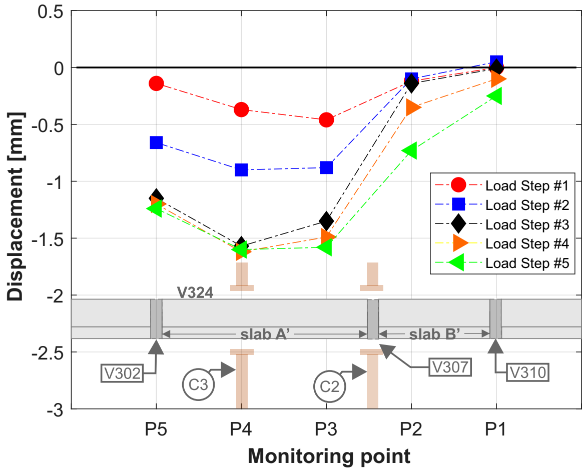

(a) V324

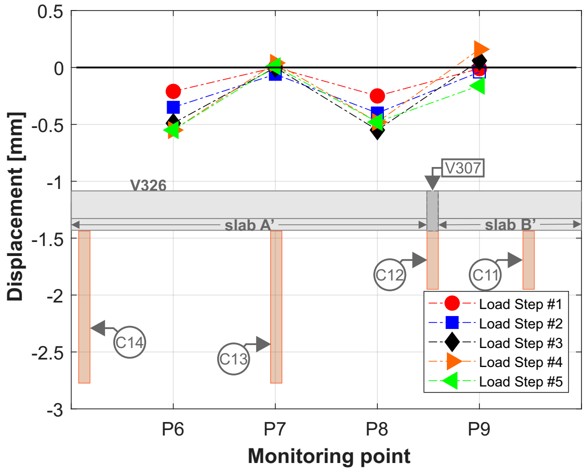

(b) V326

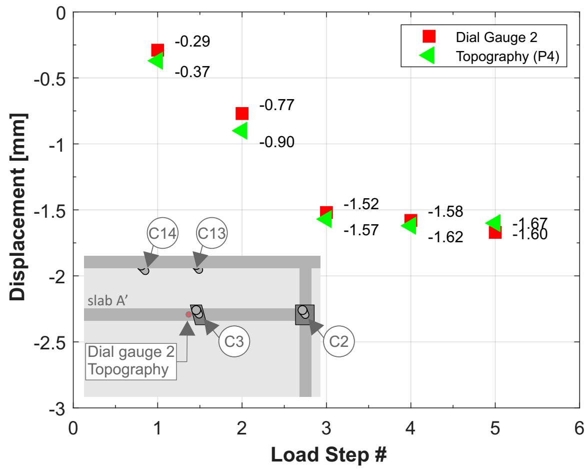

(c) Pt 4 of the second floor

Figure 6. Measured displacements in the 2^{nd} floor load test.

4.3 Numerical

The numerical simulation results were obtained from a non-linear analysis performed by TQS programme [11]. The immediate deformation was considered, since there was no time for the creep effect to become relevant.

In order to consider the deflection caused by the load test it was necessary to use one reference model. This model had only the floor's dead load acting so its vertical displacement could be obtained. Subsequently, this displacement due to the dead load was deducted from those of the load test model.

The numerical analysis was made considering the incremental effect in which the final load (water depth) was divided into 12 load steps.

These results were compared with those from the last load step of the precision geometric levelling and are presented in Figure 7.

In general, the numerical analysis have shown more ductile behavior than the precision levelling. There were identified similar displacement patterns using both methods. However, the value difference between both methods are a tenth of millimeter which can be neglected when analyzing this structure.

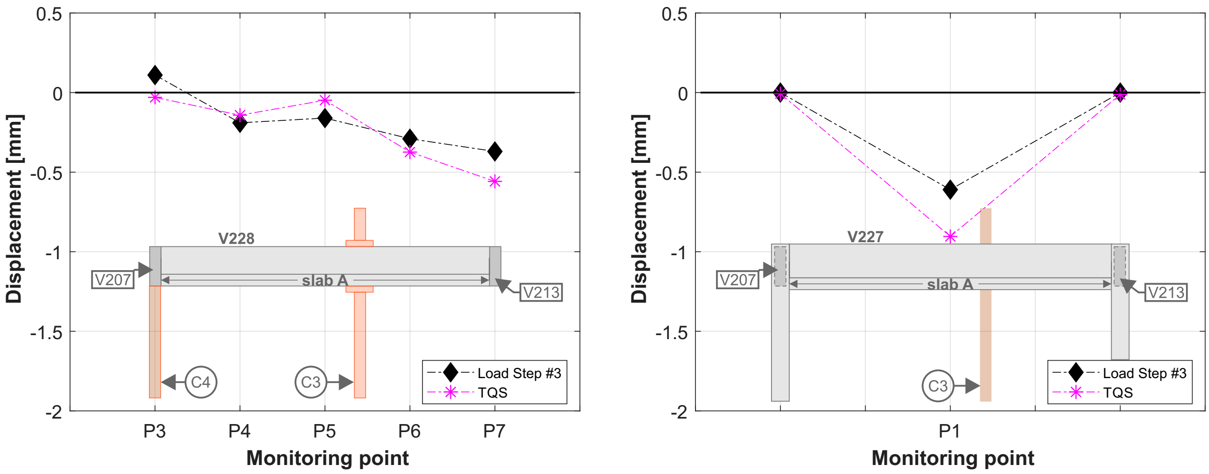

(a) 1^{st} floor load test

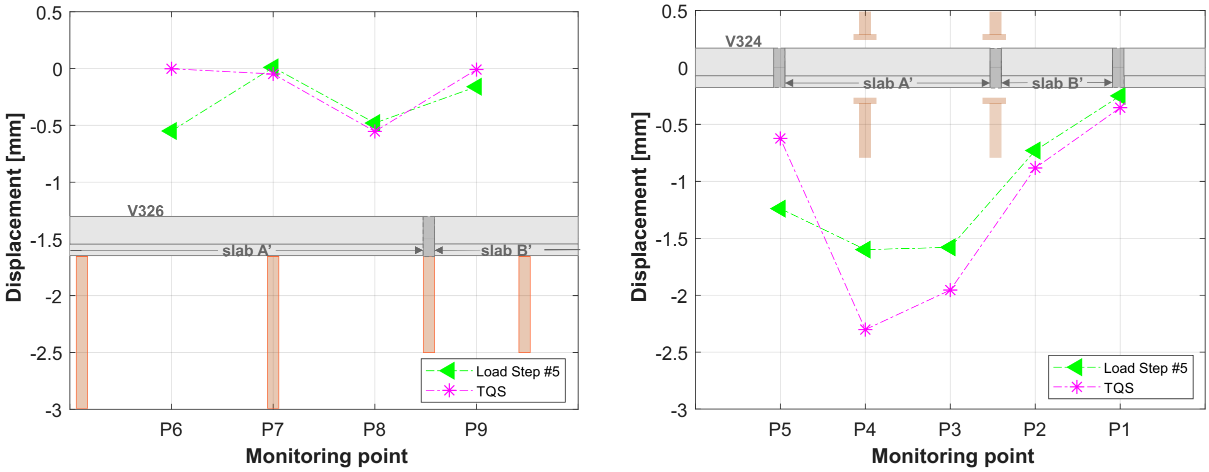

(b) 2^{nd} floor load test

Figure 7. Comparative results with numerical model.

The final displacement values of the first and second floor are presented in Tables 3 and 4, respectively. It is also indicated the serviceable limit displacement ($l/350$) due to accidental load established by the Brazilian Standard ABNT NBR 6118 [9].

In the experimental and numerical results, the displacements were way below the limit, probably due to the inclusion of new columns in the strengthening process. Additionally, the structural elements cross-section contributed for reducing the deflection, once they had higher stiffness. The slabs, for example, had 200mm thickness whereas some beams had 250x750mm section.

Table 3. Displacement limit at the first floor.

Monitoring Point	l (mm)	Vertical displacement (mm) Load Step #3	TQS	$l/350$
P1	9800	-0.61	-0.90	-28
P2	5600	-0.29	-0.23	-16
P3	-	0.11	-0.03	-
P4	5600	-0.19	-0.14	-16
P5	5600	-0.16	-0.05	-16
P6	4200	-0.29	-0.37	-12
P7	4200	-0.37	-0.56	-12
P8	5600	-0.38	-0.35	-16
P9	5600	-1.51	-2.68	-16
P9*	5600	-1.47	-2.68	-16

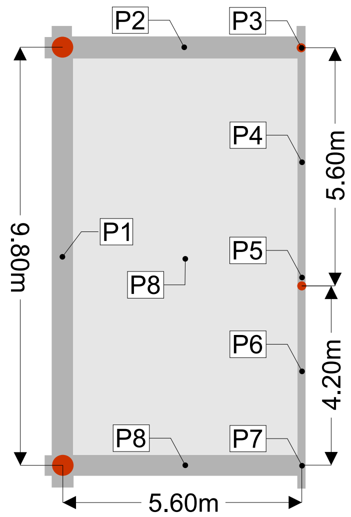

* Dial gauge measurement

Table 4. Displacement limit for at the second floor.

Monitoring Point	l (mm)	Vertical displacement (mm) Load Step #5	TQS	$l/350$
P1	8400	-0.25	-0.35	-24
P2	8400	-0.73	-0.88	-24
P3	16800	-1.58	-1.95	-48
P4	16800	-1.60	-2.30	-48
*P4	16800	-1.67	-2.30	-48
P5	16800	-1.24	-0.62	-48
P6	5600	-0.55	0.00	-16
P7	5600	-0.01	-0.04	-16
P8	8400	-0.48	-0.55	-24
P9	6050	-0.16	0.01	-17

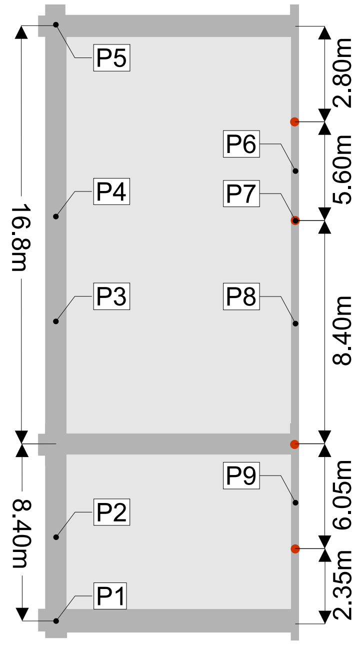

* Dial gauge measurement

Figure 8 shows the final floor displacement obtained in the load tests. An attempt was made to simulate properly the boundary conditions of the pavement given that it is mostly supported by reinforced concrete walls. For this, the entire floor was modeled and the RC wall region was considered as a column with cross section equal the wall.

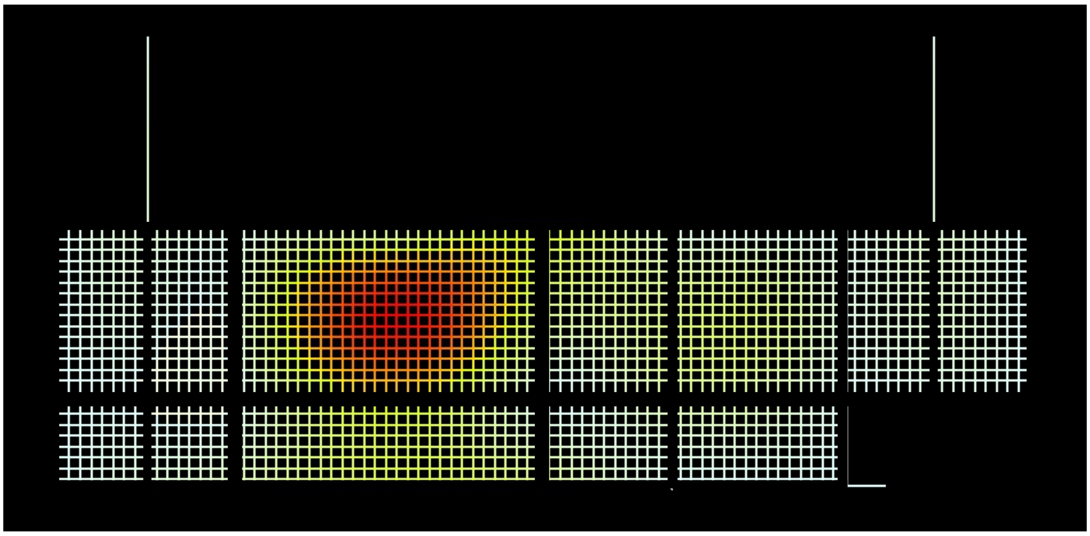

(a) 1^{st} floor load test

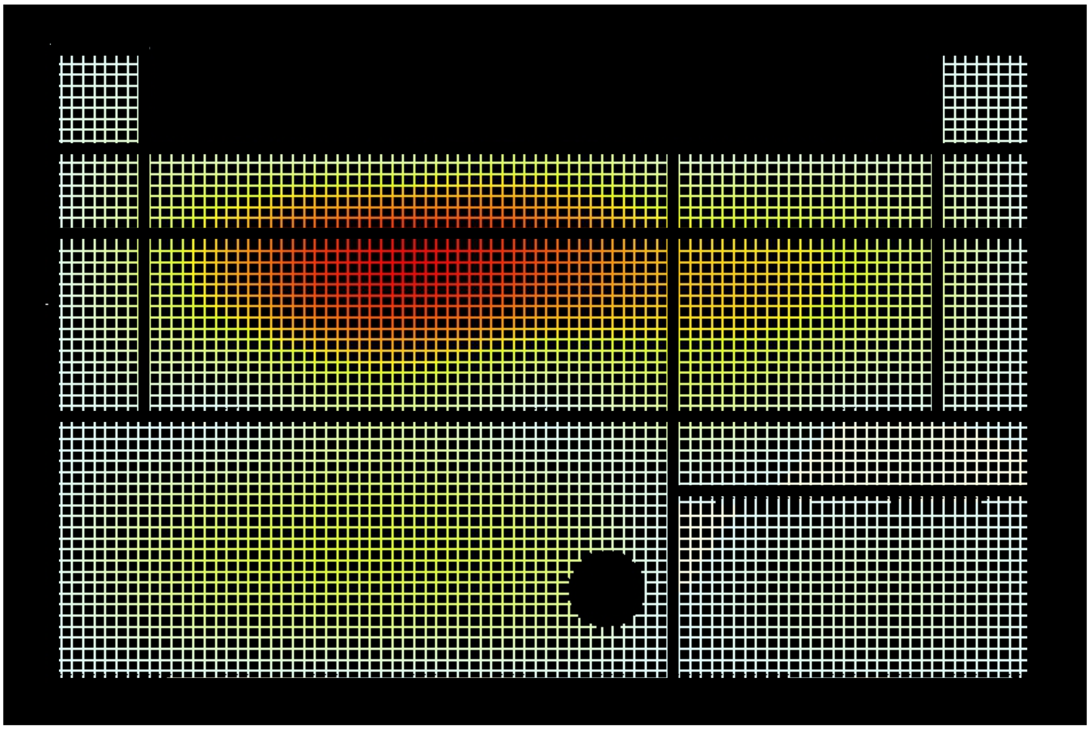

(b) 2^{nd} floor load test

Figure 8. Displacement pattern obtained through non linear analysis of TQS programme.

5 Conclusion

Despite the difficulties in modeling a structure which had previously reached a high level of solicitation, the results and displacement patterns presented a good agreement.

The dial gauges measurements showed that the use of precision geometric levelling for monitoring the displacement of structural element provided satisfactory results, since the maximum difference between them was below 0.1 millimeters (P9 and P4 on Tables 1 and 2, respectively).

In general, the numerical simulation showed similar displacement pattern as the precision geometric levelling, although a more ductile behavior was observed in the numerical models. The small differences found can be explained by approximations when choosing the point in the numerical model with the same position of the real monitoring points. In addition, the real structure suffered with the appearance of serious cracks before the load test has been performed. This might interfere in the structural behavior and it couldn't be incorporated on the numerical model.

The strengthening process which the structure was submitted included new supporting columns for the first and second floor, which reduced the effective span of the some beams. Therefore, the vertical displacements were reduced on the beams and slabs of these pavements as it was observed using the precision geometric levelling method, dial gauges and numerical analysis. It became clear that the structure meets the serviceable requirement on regions where the load tests where performed, once the displacements were way below the standard limit.

Acknowledgements

The authors would like to express their gratitude to the Coordenação de Aperfeiçoamento de Pessoal de Nível Superior (CAPES), Conselho Nacional de Desenvolvimento Científico e Tecnológico (CNPq) and the Structural Modeling and Monitoring Laboratory (LABMEM) of the University of Campinas (UNICAMP) for supporting this research. Website: `http://www.fec.unicamp.br/~labmem/`

References

[1] Napolitano, R., Liu, Z., Sun, C., & Glisic, B., 2019a. Combination of image-based documentation and augmented reality for structural health monitoring and building pathology. *Frontiers in Built Environment*, vol. 5, pp. 1–14.

[2] Chang, P. C., Flatau, A., , & Liu, S., 2003. Health monitoring of civil infrastructure. *Structural Health Monitoring*, vol. 2, pp. 257–267.

[3] Almeida, L. C., Trautwein, L. M., & Basaglia, C., 2014. Estudo das patologias de projeto e construção em uma estrutura de concreto armado. *1º Congresso Brasileiro de Patologia das Construções*, vol. 1, pp. 1–16.

[4] Araújo, T., Vieira, S., & Ribeiro, T., 2016. Analysis of structural integrity of a non-completed 28 year-old building in the city of patos de minas (mg). *J Build Rehabil*, vol. 15, pp. 1–12.

[5] Napolitano, R., Hess, M., & Glisic, B., 2019b. Quantifying the differences in documentation and modeling levels for building pathology and diagnostics. *Archives of Computational Methods in Engineering*, vol. 1, pp. 1–18.

[6] Carmo, P. O., 2003. *Patologia das construções*. UFSM. Programa de atualização profissional – CREA – RS.

[7] Helene, P. R. L., 1992. *Manual para Reparo, Reforço e Proteção de Estruturas de Concreto*. 2^a edição. São Paulo: PINI. 213 p.

[8] Souza, V. C. & Ripper, T., 2009. *Patologia, recuperação e reforço de estruturas de concreto*. 1^a edição. São Paulo: PINI. 225 p.

[9] ABNT NBR 6118, 2014. *Projeto de estruturas de concreto - Procedimento*. ASSOCIAÇÃO BRASILEIRA DE NORMAS TÉCNICAS, Rio de Janeiro.

[10] Marchena, I. P., Françoso, M. T., Almeida, L. C., & Silva, M. A., 2019. Precision geometric levelling for the control of vertical displacements in the recovery and reinforcement of concrete beam, a case study. *Revista Ingeniería de Construcción*, vol. 34.

[11] TQS Informática LTDA, 2014. *CAD/TQS Projeto Estrutural de Edifícios de Concreto Armado, Protendido, Pré-Moldados e Alvenaria Estrutural*. Visão Geral. São Paulo. 460 p.